

# Innovative PMMA/CaCO<sub>3</sub> Nanocomposites

M. Avella, M.E. Errico, G. Gentile

Istituto di Chimica e Tecnologia dei Polimeri, ICTP-CNR  
Via Campi Flegrei, 34 Pozzuoli (NA), Italy, bors@ictp.cnr.it

## ABSTRACT

PMMA based nanocomposites filled calcium carbonate nanoparticles (CaCO<sub>3</sub>) were prepared and characterized. In order to obtain a good nanoparticles dispersion and to promote polymer/nanofillers interfacial adhesion, CaCO<sub>3</sub> surface was modified by grafting poly(butylacrylate) chains. PMMA filled with unmodified nanoparticles was also prepared to evaluate the influence of the rubbery acrylic phase onto surface on the final material properties. SEM analysis performed on the fractured surface of nanocomposites revealed homogeneous and fine nanofillers dispersion. As concerning modified nanoparticles, a strong interconnection between the phases was also observed. Mechanical analysis evidenced that elastic modulus increases at high nanoparticle content while PMMA toughness is clearly influenced by the presence of the coating agent. Finally, CaCO<sub>3</sub> nanoparticles are responsible for a significant improvement of the abrasion resistance.

**Keywords:** functionalization, interfacial adhesion, mechanical properties, nanocomposites, PMMA.

## 1 INTRODUCTION

Poly(methylmethacrylate), PMMA, is an important thermoplastic finding application in many sectors such as aircraft glazing, signs, lighting, architecture, and transportation. Moreover, since PMMA is non-toxic, it could be also useful in dentures, medicine dispensers, food handling equipments, throat lamps, and lenses. Unfortunately, PMMA is characterized by poor abrasion resistance with respect to glass, thus limiting its potential use in other fields. Despite several efforts, attempts to improve PMMA scratch resistance have induced other drawbacks, such as a decrease of the impact strength.

Previous researches focused on the preparation of polymer based nanocomposites [1,2,3] have shown that properly modified calcium carbonate nanoparticles (CaCO<sub>3</sub>) are competitive, in respect to other inorganic nanofillers, to impart extraordinary properties to several thermoplastic materials (polyolefins, polyesters, polyacrylates) without strongly affecting the production costs.

The main goal of this research was to improve PMMA performance by preparing innovative PMMA based nanocomposites filled with calcium carbonate nanoparticles (CaCO<sub>3</sub>). Moreover, in order to promote polymer/nanofillers interfacial adhesion, CaCO<sub>3</sub> surface was

modified by grafting polyacrylic chains. In particular, poly(butylacrylate) (PBA), rubbery polymer, was selected as coating agent in order to improve the toughness of PMMA based nanocomposites. In fact, generally speaking, the inclusion of inorganic rigid fillers into polymer matrix induces the increase of the polymer stiffness meanwhile significantly decreasing its toughness [4]. As a matter of fact, the effect of the rubbery acrylic phase on final properties of materials was studied by means of morphological, calorimetric and mechanical analyses as well as by abrasion tests.

## 2 EXPERIMENTAL SESSION

### 2.1 Materials

Methylmethacrylate (MMA), butylacrylate (BA), dibenzoylperoxide (DBPO), vinyltrimethoxysilane (VTMS), KI, ICl, Na<sub>2</sub>S<sub>2</sub>O<sub>3</sub> 0.1 M solution, Aldrich reagent-grade product, were used without further purification. Precipitated uncoated CaCO<sub>3</sub> nanoparticles (spherical shape, 70 nm average diameter) were kindly supplied by Solvay Advanced Functional Minerals (Giraud-France).

### 2.2 CaCO<sub>3</sub> surface modification

A silane coupling agent (VTMS) was used to introduce double bonds (i.e., reactive groups) onto the surfaces of CaCO<sub>3</sub> nanoparticles. 9 g of CaCO<sub>3</sub> and 0.45 g of VTMS were suspended in 210 mL of 95% ethyl alcohol solution. The mixture was refluxed at the boiling temperature (~85°C) for 12 h under mechanical stirring. After that, the nano-CaCO<sub>3</sub> particles were centrifuged, and the precipitate was extracted with ethyl alcohol for 16 h to remove the unreacted silane. Then the modified nano-CaCO<sub>3</sub> (S-CaCO<sub>3</sub>) were air-dried at 80°C under vacuum for 24 h.

In a flask 9 g of S-CaCO<sub>3</sub> were dispersed into 72 mL of chloroform in an ultrasonic bath for 20 min at room temperature. Then the flask was put in an oil bath at 80°C and a solution of 3.6 g of BA containing 0.036 of DBPO was dropwise added. The reaction was carried out for 12 h under mechanical stirring. The final product (unextracted PBA-CaCO<sub>3</sub>) was recovered after solvent evaporation and dried overnight at 100°C under vacuum. The ungrafted PBA was removed by Soxhlet extraction with chloroform for 16 h. Finally, the recovered PBA-g-CaCO<sub>3</sub> phase was air dried at 80°C overnight.

## 2.3 PMMA/CaCO<sub>3</sub> preparation

In a flask 0.5 g (1.5 g) of PBA-g-CaCO<sub>3</sub> were added to 49.5 g (48.5 g) of MMA. The dispersion was kept for 20 min in an ultrasonic bath. After this period, 1 % by weight of DBPO (with respect to the acrylic phase) was added to the dispersion and then the flask was put in an oil bath at 80°C. This dispersion was mechanically stirred until a critical viscosity that corresponds to a prepolymerization step of the monomer. The viscous mixture was then poured into a mould and kept at 70°C for 12 h in oven. Finally, the temperature was raised to 140°C for further 12 h to complete the polymerization process. This preparation procedure was used for both uncoated and modified nanoparticles, as well as for neat PMMA.

## 2.4 Techniques

The content of the double bonds introduced onto the CaCO<sub>3</sub> surfaces by the above treatment was detected by titration. That is 0.5 g of S-CaCO<sub>3</sub>, 50 mL of chloroform, and 20 mL of ICl solution in acetic acid (0.1 M) were poured into a 150-mL flask. After stirring for 15 min, a 20 mL of KI solution (15%) was charged. Then the mixture was titrated with 0.1 M Na<sub>2</sub>S<sub>2</sub>O<sub>3</sub> solution (volume V<sub>1</sub>). The same experiment was repeated with unmodified CaCO<sub>3</sub> nanoparticles, and the necessary volume of the Na<sub>2</sub>S<sub>2</sub>O<sub>3</sub> solution used for this titration is V<sub>0</sub>. Then, the amount of the double bonds (n<sub>V<sub>TMS</sub></sub>) was calculated by the following equation:

$$n_{VTMS} = 0.5 \times (V_0 - V_1) \times 0.1 \quad (1)$$

where V<sub>0</sub> and V<sub>1</sub> are expressed in liters and 0.1 is the Na<sub>2</sub>S<sub>2</sub>O<sub>3</sub> solution concentration (mol/L).

The infrared spectra were recorded at room temperature using 64 scans, 2 cm<sup>-1</sup> resolution with a Perkin Elmer Paragon 2000 Fourier Transform Infrared (FTIR) spectrometer (Switzerland). The spectra were performed on pressed disc obtained by mixing samples (CaCO<sub>3</sub>, unextracted PBA-CaCO<sub>3</sub> and PBA-g-CaCO<sub>3</sub>) with KBr powder.

The infrared spectra were recorded at room temperature using 64 scans, 2 cm<sup>-1</sup> resolution with a Perkin Elmer Paragon 2000 Fourier Transform Infrared (FTIR) spectrometer (Switzerland). The spectra were performed on pressed disc obtained by mixing samples with KBr powder.

Thermogravimetric analysis (TGA) was performed on neat CaCO<sub>3</sub>, S- CaCO<sub>3</sub>, unextracted PBA-CaCO<sub>3</sub> and PBA-g-CaCO<sub>3</sub> nanoparticles by using a TC 10A Mettler TG equipped with a M3 analytical thermobalance, by recording the weight loss as a function of temperature. The samples were heated from 40°C to 1100°C at a scanning rate of 10°C/min in air atmosphere. The amount of total PBA (unextracted PBA-CaCO<sub>3</sub>) and the amount of PBA grafted onto CaCO<sub>3</sub> surface (PBA-CaCO<sub>3</sub>) was evaluated by comparing the related TGA traces with that of S-CaCO<sub>3</sub>.

Glass transition temperatures were evaluated by using a differential scanning calorimeter Mettler DSC-30. The samples were heated from -100 to 200°C at a scanning rate of 10°C/min. Dry nitrogen gas was purged through the cell. The glass transition temperature (T<sub>g</sub>) was determined for each sample as the temperature corresponding to the maximum of the peak obtained by the first order derivative trace of the DSC thermoanalytical curve.

Morphological analysis was performed by using a scanning electron microscope (SEM), Cambridge Stereoscan microscope model 440, on cryogenically fractured surfaces. Before the observation, samples were metallated with a gold layer.

Flexural tests were carried out at room temperature by using an Instron mechanical testing instrument (Model 1122) on unnotched samples (60 mm long, 6.0 mm wide, 3.0 mm thick). The test span was 48 mm. The cross-head speed was 1 mm/min. The elastic modulus (E) was measured.

Impact tests were performed at room temperature with an Instrumented Charpy pendulum on samples sharply notched as described as follows: first a blunt notch was obtained through a machine with a V-shaped tool and then a sharp notch 0.2 mm deep was made by a razor blade. The final value of the notch depth was measured after fracture by an optical microscope. The test span was 48 mm. The resilience (R) and the critical strain energy release rate (G<sub>c</sub>) were calculated according to the concepts of linear elastic fracture mechanics (LEFM) [5].

The abrasion tests were carried out using a Taber model 5130 abramer on neat PMMA, PMMA/CaCO<sub>3</sub> and PMMA/PBA-g-CaCO<sub>3</sub> materials. The dimensions of specimens were 5x10x10 cm. The abrasive paper, 80 grain, was applied on the Teflon rollers of the machine. The applied weight of the arms was 1000 g. Three sessions of 500 cycles were performed on the samples. The abrasion resistance was evaluated as the loss of sample weight. On all prepared samples the following experimental procedure was performed in order to evaluate the abrasion resistance of the materials.

## 3 RESULTS AND DISCUSSION

### 3.1 CaCO<sub>3</sub> modification

Generally speaking, the grafting of polymers onto the nanoparticles surface as well on classical microparticles, could remarkably improve the dispersion of the ultrafine particles in polymer matrices. This is considered to be due to the fact that grafted chains on the surface obstacle particles aggregation by increasing the affinity of particle surface towards polymers. Moreover, the presence of organic molecules onto the surface also promotes polymer/inorganic nanofiller compatibility increasing in this way the interfacial adhesion between the two nanocomposite components.

For these reasons, CaCO<sub>3</sub> nanoparticle surface was functionalised by grafting PBA chains onto it. In particular VTMS was used in order to introduce reactive groups (i.e. double bonds) onto nanoparticle. The amount of grafted silane, determined by titration, was about 1.3% by weight with respect to dried nanoparticles.

Therefore, BA phase was polymerized by thermal decomposition of the organic peroxide in presence of endcapped double bonds silane modified nanoparticles (S-CaCO<sub>3</sub>) in order to build up grafted polyacrylate chains onto nano-CaCO<sub>3</sub> (PBA-g-CaCO<sub>3</sub>). After the extraction of PBA homopolymer, FT-IR spectroscopy was carried out on modified nanopowders confirming the presence of PBA chains grafted onto nanofiller surface, Figure 1.

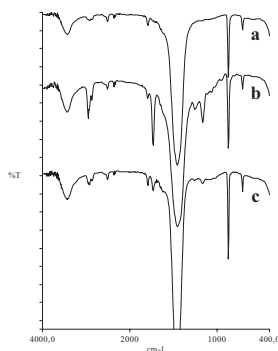


Figure 1: FTIR spectra of:  
a) neat CaCO<sub>3</sub> nanoparticles; b) unextracted PBA-CaCO<sub>3</sub> nanoparticles; c) PBA-g-CaCO<sub>3</sub> nanoparticles.

The amount of PBA homopolymer and grafted PBA was evaluated by TGA measurements. This analysis revealed that the weight ratio grafted PBA/CaCO<sub>3</sub> was 2.9%.

The DSC thermograms of the PBA-g-CaCO<sub>3</sub> nanoparticles underlined an increase of the PBA T<sub>g</sub> value of about 15°C compared to neat PBA (-60°C). This increase can be attributed to the fact that the polyacrylic chains are anchored to the calcium carbonate surface thus reducing the PBA chains mobility.

### 3.2 PMMA/CaCO<sub>3</sub> nanocomposites

PMMA based nanocomposites filled with 1 and 3% by weight of PBA-g-CaCO<sub>3</sub> nanoparticles were prepared by in situ polymerisation. PBA-g-CaCO<sub>3</sub> were dispersed into MMA phase and the polymerisation was induced by thermal decomposition of DBPO (1 wt % with respect to MMA). As detailed described into the experimental session, the in situ polymerisation process was carried out in two steps. During the first step, carried out under mechanical stirring, the low mixture viscosity allowed the fine nanoparticle dispersion. During the polymerisation, the growing PMMA chains contribute to increase the viscosity of the medium thus assuring the *freezing* of the obtained nanofiller dispersion. In the last step, performed in the

oven, the PMMA polymerisation was completed. The same procedure was used to prepare PMMA filled with 3% by weight of neat CaCO<sub>3</sub> in order to evaluate the influence of the coating agent on final nanocomposite properties.

In order to evaluate nanofiller dispersion into PMMA and the interfacial adhesion between the two components, morphological analysis was performed on fractured surface of nanocomposites. This analysis revealed that in situ polymerization methodology can provide a useful method of nanocomposite preparation with the achievement of good nanoparticle dispersion. Furthermore, as concerning PBA-g-CaCO<sub>3</sub> nanoparticles, a strong interconnection between the phases was also evidenced. This strong interconnection was also confirmed by the results obtained by DSC analysis performed on compression moulded nanocomposite samples. In fact, the T<sub>g</sub> of poly(butylacrylate) in nanocomposites containing 1 and 3 wt % of PBA-g-CaCO<sub>3</sub> undergoes to a further shift from -45°C, the glass transition value of PBA in PBA-g-CaCO<sub>3</sub> nanoparticles, up to 0°C. This significant increase can be explained by considering that the strong PMMA/PBA-g-CaCO<sub>3</sub> interfacial adhesion achieved is responsible for a restricted chain mobility of the PBA phase. In Table 1 DSC results are reported.

As concerning nanocomposites containing PBA-g-CaCO<sub>3</sub> nanoparticles, PMMA T<sub>g</sub> values appear almost unchanged with respect to neat PMMA, whereas the presence of unmodified CaCO<sub>3</sub> is responsible for a strong increase (up to 18°C) of the T<sub>g</sub> value. In the latter case the rigid nature of the filler and its good dispersion justify the increase of the PMMA chain stiffness. As concerning nanocomposites containing PBA-modified CaCO<sub>3</sub> nanoparticles, the general tendency to increase the stiffness attributed to a homogeneously dispersed rigid filler is compensated by the presence of the rubbery interfacial PBA phase. This result perfectly agrees with the fact that the interphase plays a critical role in nanocomposites so that they are often defined as interfacial composites [6,7].

% CaCO <sub>3</sub> content	T <sub>g</sub> (PBA) (°C)	T <sub>g</sub> (PMMA) (°C)
0	-	105
3% CaCO <sub>3</sub>	-	123
1% PBA-g-CaCO <sub>3</sub>	0	104
3% PBA-g-CaCO <sub>3</sub>	- 5	108

Table 1: Glass transition temperature values of neat PMMA and PMMA-based nanocomposites.

Results of mechanical analysis are resumed in Table 2 and can be summarized as follows: the elastic modulus increases up to 10% with respect to neat PMMA value as concerning nanocomposite containing unmodified nanoparticles, while this improvement is less pronounced for PMMA/PBA-g-CaCO<sub>3</sub> materials. In this latter case, the moderate increase, recorded only at high nanoparticle content, can be attributed to the presence of the rubbery polyacrylic phase grafted onto nanoparticle surface.

The toughness of nanocomposites was evaluated at low and

high deformation rate. It is generally accepted that the presence of a rigid filler could deteriorate the toughness of polymeric matrix while a rubbery phase could substantially improve this property [8]. As a matter of fact, in this research the grafting of PBA onto nanoparticle surface was performed to mitigate the possible negative effect attributable to the rigid filler. In fact, as it can be observed in Table 2, both the resilience (R) and the critical strain energy release rate ( $G_c$ ) significantly decrease in presence of unmodified  $\text{CaCO}_3$  nanoparticles. Nevertheless, the addition of PBA-g- $\text{CaCO}_3$  allows not only to undeteriorate the PMMA toughness but even permits to increase up to 20%  $G_c$  value. It is important to underline that no reduction of the elastic modulus of the material was observed in correspondence of such an increase, as generally occurs.

% $\text{CaCO}_3$ content	E (MPa)	R ( $\text{kJ/m}^2$ )	$G_c$ ( $\text{kJ/m}^2$ )
0	2115	0.76	1.78
3% $\text{CaCO}_3$	2336	0.55	1.58
1% PBA-g- $\text{CaCO}_3$	2055	0.80	2.3
3% PBA-g- $\text{CaCO}_3$	2233	0.77	2.3

Table 3: Mechanical parameters of neat PMMA and PMMA-based nanocomposites.

The abrasion resistance of a solid is defined as its ability to withstand the progressive removal of material from its surface as a result of mechanical action of a rubbing, scraping, or erosion [9]. Abrasion resistance is the key factor in the wear process of a material. Usually, abrasion reduces the usability of the affected solid and hence low abrasion resistance is a very important drawback that modern products must overcome. Abrasion occurs in contact situations in which direct physical contact occurs between two surfaces, and one of the surfaces is considerably harder than the other. The asperities of the harder surface press into the softer surface, with plastic flow of the softer surface occurring around the asperities from the harder surface, which removes the softer material by the combined effect of *microploughing*, *microcutting* and *microcracking* [10]. PMMA is characterized by a low abrasion resistance. In particular, its wear is initiated by formation of surface cracks parallel to the sliding direction as a result of a high frictional coefficient. This latter is probably due to the presence of polar groups along the backbone chains, which result in high molecular cohesion. In Table 3 results of abrasion tests are summarized. The presence of nanoparticles strongly improves abrasion resistance of PMMA. In fact, nanocomposites show an improvement of this property up to 50%, even at low nanoparticle content. Moreover, clearly, this improvement is not a function of the coating agent. This result can be explained considering that nanoparticles, homogeneously dispersed into PMMA, support part of the applied load and, in this way, the penetration into the polymer is reduced.

% $\text{CaCO}_3$ content	Weight loss ( $\text{mg/cm}^2$ )
0	42.0
3% $\text{CaCO}_3$	20.2
1% PBA-g- $\text{CaCO}_3$	26.6
3% PBA-g- $\text{CaCO}_3$	20.5

Table 3: Abrasion test results of neat PMMA and PMMA-based nanocomposites, measured as weight loss.

## 4 CONCLUSIONS

PMMA based nanocomposites filled with unmodified and PBA-modified calcium carbonate nanoparticles were prepared by in situ polymerization methodology. Morphological analysis allowed to assess that this preparation procedure is a useful method to achieve a good nanoparticle dispersion. The grafting of PBA onto nanoparticle surface induces a strong interconnection between the phases. Mechanical analysis underlined that the presence of this rubbery phase permits an improvement of the toughness of nanocomposites without negatively influencing the PMMA stiffness, whereas unmodified nanoparticles induce a significant deterioration of PMMA toughness. Finally, the presence of nanoparticles strongly improves the abrasion resistance of the polymeric matrix, independently from the presence of the nanoparticle coating agent.

## REFERENCES

- [1] C.M. Chan, J. Wu, X. Li, Y.K. Cheung, *Polymer* 43(10), 2981, 2002.
- [2] M.L. Di Lorenzo, M.E. Errico, M. Avella, J. Mater. Sci. 37(11), 2351, 2002.
- [3] M. Avella, M.E. Errico, E. Martuscelli, *Nanoletters* 1(4), 213, 2001.
- [4] K. Friedrich, "Application of Fracture Mechanics to Composite Materials", Elsevier, "Composite Materials Series, Vol. 6, USA, 1991.
- [5] J.C. Williams, "Fracture Mechanics of Polymers", John Wiley & Sons, New York, 1984.
- [6] G.M. Kim, D.H. Lee, B.J. Hoffmann, G. Stoppelmann, *Polymer* 42, 1095, 2001.
- [7] T.S. Creasy, Y.S. Kang, *J. Thermoplas. Compos. Mater.* 17, 205, 2004.
- [8] M. Abbate, E. Martuscelli, P. Musto, G. ragosta, *Die Ang. Makr. Chem.* 246, 23, 1997.
- [9] H. Czichos, "Introduction to Friction and Wear" in "Friction and Wear of Polymer Composites", K. Friedrich editor, Elsevier, New York, 1986.
- [10] K.H. Zum Ganhr, *Met. Prog.* 9, 46, 1979.